Foot pressure distribution in White Rhinoceroses (*Ceratotherium simum*) during walking

Olga Panagiotopoulou [Corresp., 1] , Todd C Pataky [2] , John R Hutchinson [Corresp. 3]

[1] Monash Biomedicine Discovery Institute, Department of Anatomy and Developmental Biology, Moving Morphology & Functional Mechanics Laboratory, Monash University, Clayton, Victoria, Australia

[2] Department of Human Health Sciences, Kyoto University, Kyoto, Japan

[3] Department of Comparative Biomedical Sciences, Structure and Motion Laboratory, Royal Veterinary College, Hatfield, United Kingdom

Corresponding Authors: Olga Panagiotopoulou, John R Hutchinson
Email address: olga.panagiotopoulou@monash.edu, JHutchinson@rvc.ac.uk

White rhinoceroses (*Ceratotherium simum*) are odd-toed ungulates that belong to the group Perissodactyla. Being second only to elephants in terms of large body mass amongst extant tetrapods, rhinoceroses make fascinating subjects for the study of how large land animals support and move themselves. Rhinoceroses often are kept in captivity for protection from ivory poachers and for educational/touristic purposes, yet a detrimental side effect of captivity can be foot disease (i.e. enthesopathies and osteoarthritis around the phalanges). Foot diseases in large mammals are multifactorial, but locomotor biomechanics (e.g. pressures routinely experienced by the feet) surely can be a contributing factor. However, due to a lack of *in vivo* experimental data on rhinoceros foot pressures, our knowledge of locomotor performance and its links to foot disease is limited. The overall aim of this study was to characterize peak pressures and centre of pressure trajectories in white rhinoceroses during walking. We asked two major questions. First, are peak locomotor pressures the lowest around the fat pad and its lobes (as in the case of elephants)? Second, are peak locomotor pressures concentrated around the areas with the highest reported incidence of pathologies? Our results show a reduction of pressures around the fat pad and its lobes, which is potentially due to the material properties of the fat pad or the fact that our rhinoceros subjects avoided "heel" contact at impact. We also found an even and gradual concentration of foot pressures across all digits, which may be a by-product of the more horizontal foot roll-off during the stance phase. While our exploratory, descriptive sample precluded hypothesis testing, our study provides important new data on rhinoceros locomotion for future studies to build on, and thus impetus for improved implementation in the care of captive/managed rhinoceroses.

2   **Title**: Foot pressure distribution in White Rhinoceroses (*Ceratotherium simum*) during walking.

3   **Authors**: Olga Panagiotopoulou[1], Todd C Pataky[2], John R Hutchinson[3]

4   1.   Monash Biomedicine Discovery Institute, Department of Anatomy and Developmental Biology,
5   Moving Morphology & Functional Mechanics Laboratory, Monash University, Victoria,
6   Australia
7   2.   Department of Human Health Sciences, Kyoto University, Kyoto, Japan
8   3.   Department of Comparative Biomedical Sciences, Structure and Motion Laboratory, The Royal
9   Veterinary College, Hatfield, UK

13   Corresponding authors:

14   Dr Olga Panagiotopoulou (olga.panagiotopoulou@monash.edu)

15   Professor John R Hutchinson (jhutchinson@rvc.ac.uk)

18 **Abstract**

19 White rhinoceroses (*Ceratotherium simum*) are odd-toed ungulates that belong to the group
20 Perissodactyla. Being second only to elephants in terms of large body mass amongst extant tetrapods,
21 rhinoceroses make fascinating subjects for the study of how large land animals support and move
22 themselves. Rhinoceroses often are kept in captivity for protection from ivory poachers and for
23 educational/touristic purposes, yet a detrimental side effect of captivity can be foot disease (i.e.
24 enthesopathies and osteoarthritis around the phalanges). Foot diseases in large mammals are
25 multifactorial, but locomotor biomechanics (e.g. pressures routinely experienced by the feet) surely can
26 be a contributing factor. However, due to a lack of *in vivo* experimental data on rhinoceros foot pressures,
27 our knowledge of locomotor performance and its links to foot disease is limited. The overall aim of this
28 study was to characterize peak pressures and centre of pressure trajectories in white rhinoceroses during
29 walking. We asked two major questions. First, are peak locomotor pressures the lowest around the fat
30 pad and its lobes (as in the case of elephants)? Second, are peak locomotor pressures concentrated around
31 the areas with the highest reported incidence of pathologies? Our results show a reduction of pressures
32 around the fat pad and its lobes, which is potentially due to the material properties of the fat pad or the
33 fact that our rhinoceros subjects avoided "heel" contact at impact. We also found an even and gradual
34 concentration of foot pressures across all digits, which may be a by-product of the more horizontal foot
35 roll-off during the stance phase. While our exploratory, descriptive sample precluded hypothesis testing,
36 our study provides important new data on rhinoceros locomotion for future studies to build on, and thus
37 impetus for improved implementation in the care of captive/managed rhinoceroses.

38

39 **Introduction**

40 Over millions of years of evolution, the feet of rhinoceroses have had to change with other alterations of
41 limb morphology, locomotor behaviour, body size, habitat and more (e.g. Prothero, 2005; Stilson et al.,
42 2016). Extant rhinoceroses include the second largest (after elephants) extant terrestrial mammals, with
43 body masses in the White rhinoceros reaching up to 3600 kg (Groves, 1972; Hillman-Smith et al., 1986;
44 Owen-Smith, 1992). Thus in large rhinoceroses locomotor stresses might be considerable if not well-
45 controlled, imposing severe biomechanical constraints on form and function (Alexander and Pond, 1992).
46 Contrary to the feet of elephants, which bear five functional digits and "predigits" (Hutchinson et al., 2011;
47 Mariappa, 1986; Neuville, 1935; Weissengruber et al., 2006), rhinoceros feet have three digits (numbered
48 II-IV) terminating in horns/hooves (Prothero, 2005; Regnault et al., 2013) and no supportive "predigits". Of
49 the three digits, digit II and IV respectively dominate the medial and lateral aspects of the foot, whilst digit
50 III is the central and largest of all. Each digit consists of three phalanges (proximal, medial and distal) and
51 the foot caudally and centrally is enclosed in a fat pat. The bi-lobed fat pad is structurally similar but smaller
52 in size to elephant fat pads and expands when compressed (von Houwald, 2001). This structure potentially
53 helps to evenly distribute locomotor stresses across the sole of the foot, as in the case of elephants
54 (Panagiotopoulou et al., 2012, 2016). Overall, the morphology of rhinoceros feet is fairly symmetrical from
55 medial to lateral, unlike the feet of elephants which are more robust laterally (e.g. digits III-V).

56 Considering that large mammals' feet support their body mass during gait, understanding healthy foot
57 function is important for understanding healthy gait. This is particularly imperative in view of documented
58 rhinoceros foot pathologies (Dudley et al., 2014; Flach et al., 2003; Galateanu et al., 2013; Harrison et al.,
59 2011; Jacobsen, 2002; Jones, 1979; Regnault et al., 2013; Von Houwold, 2001; Von Houwald and
60 Guldenschuh, 2002; Von Houwold and Flach, 1998; Zainuddin et al., 1990). Previous research on museum
61 specimens found a high occurrence of enthesopathies and osteoarthritis on the phalanges of rhinoceros feet
62 (Regnault et al., 2013)-- of the 81 feet from 27 rhinoceroses studied, 54 feet from 22 individuals exhibited
63 osteopathologies (Dudley et al., 2014). Surprisingly, limb osteopathologies have remained common in
64 rhinocerotid species across their evolution but increasing with estimated body mass. This is consistent with
65 tradeoffs and compromises between large size, cursorial/mediportal morphology or athletic capacity, and

66   limb health (Stilson et al., 2016).

67   Many factors can cause foot disease in large mammals, but previous research in elephants has linked foot
68   disease with obesity, space limitations and the time the animals spent walking or standing on hard
69   (unnatural) surfaces (Csuti et al., 2001; Fowler and Mikota, 2006; Miller et al., 2016). Our prior studies
70   proposed that elephants normally have high pressures laterally, on digits III-V (Panagiotopoulou et al., 2012,
71   2016), congruent with where elephants tend to exhibit greater incidences of osteopathologies (Regnault et
72   al., 2017). In contrast, there are almost no *in vivo* studies of locomotion in rhinoceroses (e.g. Alexander and
73   Pond, 1992), in any aspects including the pressures experienced by the feet. Based on the roughly equivalent
74   occurrence of osteopathologies across rhinoceros digits II-IV (Regnault et al., 2017), we expect that
75   pressures would be evenly distributed across these digits too, and for pressures to be low on the fat pad
76   lobes, without the mediolateral asymmetry of pathologies or pressures observed in elephant feet.

77   In this pilot study, we describe *in vivo* locomotor foot pressures and centre of pressure trajectories (COP) in
78   three white rhinoceroses (*Ceratotherium simum*) during walking. Our limited sample size does not allow us
79   to conduct hypothesis testing on foot pressure magnitudes. However, we were able to conduct preliminary,
80   qualitative evaluation of our two exploratory hypotheses, for future studies to expand on:

81   Hypothesis I. Peak locomotor pressures will be the lowest in the central and caudal parts of the foot at the
82   locations of the fat pad and its lobes. This is expected from a dynamic interaction of behavioural walking
83   preferences (manifested in COP) and the compliant properties of the fat pad, as we have previously observed
84   in elephants (Panagiotopoulou et al., 2012, 2016).

85   Hypothesis II. Peak locomotor pressures will be concentrated equally around the horns/hooves and
86   phalangeal pads of all digits (II-IV), which correspond to the overlying bony areas with the highest evidence
87   of osteoarthritis and similar pathologies (Regnault et al, 2013), without a strong tendency for more lateral
88   prevalence of pathology.

89

90   **Methods**

91   Subjects

92   Four adults and a juvenile captive southern White Rhinoceros (*Ceratotherium simum*) from Colchester Zoo
93   (Colchester, UK) participated in the study, however only data from two adults and one juvenile could be
94   used for further analyses (Table 1). The body masses of the subjects were estimated by the zoo keepers
95   using the zoo's records. Zoo keepers and veterinarians gave clinical consent for the study and all animal
96   participants were healthy. The study was approved by The Royal Veterinary College's Animal Ethics
97   Committee (approval number URN 2010 1052).

98   Data collection

99   A 5 m walkway was constructed in a crush area in the rhinoceros enclosure (Figure 1A). A 3 m long and
100   0.4 m wide foam pad was laid at the beginning of the walkway and was followed by a 1.0 x 0.4 m pressure
101   plate (fitted with 8192 sensors, 2.05 sensors cm^{-2}) (Footscan; RSscan, Olen, Belgium), and a 1 m length of
102   foam pad. The walkway was covered with a 0.3 mm thick rubber mat to prevent the animals from
103   recognising the location of the pressure plate. Reflective tape was placed on the rhinoceros hip and shoulder
104   to calculate walking speeds using a Sony HDR (Sony, London, UK) high definition video camera. The
105   camera was placed perpendicular to and at a 2 m distance from the walkway. Camera and pressure plate
106   sampling frequencies were respectively 25 Hz and 250 Hz. The pressure plate was calibrated using a known
107   weight (~95 kg human standing on the plate) as per manufacturer's instructions. While we do report
108   absolute pressure magnitudes, the main outcome of interest was the relative (i.e. within-foot) pressure
109   distribution, as this reflects foot functionality. Absolute pressure errors are unexpected to affect relative

110   pressure values. The rhinoceros were guided over the walkway using food as encouragement, an average
111   of 20 times each. Trials with obvious acceleration and deceleration (as judged by video) during data
112   collection were excluded from further analysis (Panagiotopoulou et al., 2012, 2016). Animal discomfort
113   was kept to the minimum by stopping data collection when animals appeared disengaged.

114   Data processing

115   Data analysis protocols were similar to Panagiotopoulou et al., (2012, 2016), implanted in Canopy v. 2.1.8
116   using SciPy v. 0.19, NumPy 1.11.3 and Matplotlib 2.0 (Enthought Inc., Austin, TX, USA). In brief, the raw
117   pressure data (x, y, time) of the individual footsteps were exported from the Footscan system, isolated
118   algorithmically using spatio-temporal gaps between clusters of non-zero pressure voxels and were assessed
119   for spatial and temporal completeness as per Panagiotopoulou et al., (2012, 2016). Individual images
120   representative of spatio-temporally complete footsteps were manually identified as fore/hind, right/left;
121   spatially scaled by a factor of 1.5, using bilinear interpolation to compensate for the non-square
122   measurement grid of the RSscan system (7.62 x 5.08 mm, manufacturer specified); and spatially registered
123   within subjects and feet (see Panagiotopoulou et al., (2012)). Following scaling and registration, nine
124   anatomically homologous regions of interest (ROIs) were selected on the mean images for each foot as per
125   Panagiotopoulou et al., (2012, 2016), and peak pressures (N cm^{-2}) of the whole stance phase were extracted
126   from a three-pixel radius using a Gaussian kernel mean window with a standard deviation of one pixel.
127   ROIs 1-3 respectively represented the horns of digits II-IV, ROIs 4-6 represented the (inter)phalangeal pads
128   of digits II-IV respectively, ROI 7 represented the caudal most ("heel") aspect of the sole and ROIs 8-9
129   were respectively placed on the medial and lateral footpads of the sole (Figure 1B). Centre of pressure
130   trajectories (COP) were computed as the pressure-weighted image centroids' time series after thresholding
131   the images at 0.5 N cm^{-2}. Due to the limited number of subjects and steps, the dependent variables were
132   not tested for significance. This was a preliminary, qualitative study of rhinoceros foot function during gait,
133   so we neither derived nor tested a null hypothesis.

134

135   **Results**

136   The mean walking speed of all three subjects was 0.53 ms^{-1} (Table 1), which corresponded to a mean Froude
137   number (Alexander and Jayes, 1983; Fr = velocity^2 * [9.81 ms^{-2} * shoulder height]$^{-1}$) of 0.013, consistent
138   with a slow walk. The peak pressure data per ROI, subject and feet are shown in Table 1. All peak pressure
139   data are in Supplementary Data 1. Raw pressure data including all trials and steps are available on Figshare
140   (Panagiotopoulou et al., 2019). The mean peak pressure values for the adult subjects 1 and 3 and all feet
141   were respectively 22 N cm^{-2} and 18 N cm^{-2}, whilst the mean peak pressure values of the juvenile subject 2
142   were 0.9 N cm^{-2}. The mean peak pressure values for both adult subjects and all feet (20 N cm^{-2}) were
143   respectively 4.7 and 2.8 times lower than those previously recorded on African (94.6 N cm^{-2}) and Asian
144   elephants (56.7 N cm^{-2}) during walking (Panagiotopoulou et al., 2012, 2016). The Asian elephant data were
145   collected using the same RSscan system as in this study, yet the African elephant pressure data were
146   collected using a lower resolution system (Zebris Medical GmbH, Biomechanix, Munich) with 100 Hz
147   sampling frequency, sensors resolution of ½ inch and sensor size of 1.27 cm x 1.27 cm, so the present
148   study's data are not comparable with those prior data. Our data showed that, similar to elephants and other
149   quadrupeds, the forefeet had higher mean pressure magnitudes than the hindfeet for all subjects (Table 1).

150   Contrary to elephants (Panagiotopoulou et al., 2012, 2016), the rhinoceroses' foot pressures did not follow
151   a consistent pattern between feet. The forefeet for adult subject 3 and the juvenile rhinoceros (subject 2)
152   showed higher pressures around the horn of digits II (ROI 1), III (ROI 2) and IV (ROI 3). Intermediate
153   pressures were recorded around the phalangeal pads of digits II-IV and the lowest pressures around the fad
154   pad (ROIs 7-9) (Figures 2, 3 & 4). The highest median foot pressures for the right forefeet of all three
155   rhinoceroses were at the horn of digits III and IV, corresponding to ROIs 2 and 3 (Figures 2 & 4). The
156   lowest median peak pressures were recorded around the fat pad; nevertheless, median peak pressures around

157 the phalangeal pads of all digits were very low. Median pressures for the left hindfeet were the highest for
158 the horn of digit II, followed by ROIs 2 and 3 (Figures 2 &5). Intermediate median pressures were recorded
159 at ROIs 4, 5 and 7 and the lowest peak pressures were computed at ROI 8. Regardless, median peak pressure
160 differences between ROIs 2-9 were minimal (Figure 2 & Supplementary Data 1.) Median peak pressures
161 for the hindfeet of the two adult subjects (subject 1 and 3) gave the highest median peak pressures at the
162 horn of digit II (ROI 1) and intermediate pressures at ROIs 2-4 (Figures 2 & 6). The lowest peak pressures
163 were found at ROIs 5-9.

164 The COP trajectories for all time frames, animal participants and feet are shown in supplementary Figures
165 S1- S8. Most COP traces began at the medial aspect of the foot caudally to the interphalangeal pad of digit
166 II or at the medial footpad of the sole, then shifted caudally around the heel aspect of the sole and finally
167 passed cranially through digit III by toe-off. Contrary to this caudo-medial and centrally-focused pressure
168 pattern, pressure traces in two trials for the hind leftfoot started laterally on digit IV before shifting caudo-
169 cranially and through digit III by toe-off. Thus there was some unusual variability in our subjects' COP
170 traces during normal locomotion.

171

172 **Discussion**

173 Overall, we found reduction of peak pressures around the fat pads of the feet, qualitatively supporting our
174 hypothesis I that, like in elephants, rhinoceros fat pads may keep locomotor pressures low due to their
175 compliance. Whilst our quantitative results showed variation in peak foot pressures across feet, we recorded
176 the highest peak pressures around the horn and phalangeal pads of all digits, yet this signal was not as strong
177 for the left hindfoot (Figure 2). Such variations may be due to the ROI method used for data analysis.
178 Although the ROI approach is a widely used technique for the estimation of peak pressure magnitudes
179 sampled from specific anatomical regions, it overlooks variability within regions, assuming that all regions
180 are functionally independent. We have previously shown a significant interaction between the topology of
181 the ROIs and pressure magnitudes in elephants (Panagiotopoulou et al., 2016). Variation in peak pressures
182 between ROIs may also have a biological importance considering that the left hindfoot sometimes showed
183 a lateral-caudal-central roll off pattern, but we remain conservative with any biological conclusions due to
184 our experimental and sample size limitations.

185 The general COP trajectories in our rhinoceros subjects were similar to elephants in being linear during the
186 final half of stance phase rather than sigmoidal as in humans (Lord et al., 1986) and bonobos (Vereecke et
187 al., 2003). However, contrary to elephants, our rhinoceros subjects loaded the medial part of the foot at
188 impact and then shifted their load centrally during mid-stance prior to toe-off via their central digit. Reasons
189 for this apparent preference to avoid "heelstrike", and the strongly medially-biased COP pattern in our
190 subjects early in stance phase, remain unclear. Nevertheless, the variability of COP patterns is cause for
191 caution in attributing this pattern to all rhinoceroses until more such data can be obtained and compared.
192 However, this medial bias early in stance phase does, tantalizingly, fit with the pattern observed by von
193 Houwald (2001) in Indian rhinoceroses, in which the medial angle of the foot tended to develop cracks and
194 similar wear earlier than other regions. Hints at other unusual COP patterns – or perhaps subject variability
195 or measurement error – in large mammals (e.g. hippopotamus and tapir COP traces in Figure 1 of
196 Michilsens et al., 2009) are further cause for caution and future analyses. More detailed studies of cows,
197 for example (van der Tol et al., 2002, 2003, 2004) indicate further apparent interspecific variation, such as
198 cows tending to have larger pressures on their lateral (vs. medial) horns (i.e. claws), and having their
199 forefeet more evenly loaded throughout stance phase vs. hindfeet with pressure magnitudes that shift from
200 lateral at heelstrike to medial at toe-off.

201 Due to this variation in rhinoceroses' foot pressures and COP trajectories, locomotor patterns are important
202 for assessing peak pressure distributions qualitatively. The peak pressure "heat maps" for all subjects and
203 steps shown in Figures 3-6 indicated a clear concentration of peak pressures around the horn and phalangeal

204 pads of all three digits. These results tentatively support our hypothesis II-- that peak pressures are evenly
205 distributed, rather than biased toward the central and lateral digits, which corresponds to the relatively even
206 distribution of osteopathologies across digits II-IV (Regnault et al., 2013). An even distribution of peak
207 pressures across all three digits might be a by-product of the horizontal position of the foot at impact as
208 manifested by the COP traces (i.e. avoidance of heelstrike). Regardless, large animals such as elephants
209 and rhinoceroses clearly use enlarged foot contact areas to protect the digits from peak pressures that
210 otherwise could cause tissue damage (Chi and Roth, 2010; Michilsens et al., 2009).

211 It is also interesting that forefoot pressures were normally higher in our three subjects, and forefoot
212 osteopathologies tend to be more common than hindfoot osteopathologies (Regnault et al., 2013)—although
213 one study found more chronic foot disease overall in the hindfeet, rather than forefeet, for a sample of One-
214 horned rhinoceroses (von Houwald and Flach, 1998). The latter study posited some biomechanical factors
215 that may underlie foot pathologies, including toe horn-cracking, shearing forces on the middle toe, low
216 friction causing low wear and overgrowth of the middle toe horn, which could inspire future studies building
217 on this one. Regardless, these patterns are opposite those tentatively identified for elephants sampled by
218 Regnault et al., (2017) — they found no clear forefoot vs. hindfoot differences in osteopathologies despite
219 some evidence for higher pressures on elephant forefeet (Panagiotopoulou et al., 2012, 2016). It is tempting
220 to speculate that the more similar morphology and presumably function of all four rhinoceros feet compared
221 with the disparate morphology of elephant fore- vs. hindfeet may explain these discrepancies, but such
222 speculations demand cautious future analysis.

223 Many factors account for osteopathologies such as congenital, developmental, metabolic, diet, age,
224 traumatic injuries (summarised in Galateanu et al., 2013). However, captivity in enclosures with limited
225 space for the animals to remain athletic, and exposure to hard concrete for long hours may exacerbate foot
226 disease even if not the primary cause. To better understand foot pressures in rhinoceroses and the links to
227 foot disease, more *in vivo* locomotor data are required; ideally from multiple species and management
228 regimes. Von Houwald (2001) speculated that wild rhinoceroses walk on their soles (phalangeal pads)
229 whereas captive rhinoceroses walk more on their fat pads. It would be fascinating to investigate this
230 possibility using pressure pad analyses in the future.

231 Contrary to elephants that can easily be trained to walk over a walkway lined with pressure plates using
232 food as encouragement, rhinoceroses are seldom well-trained, so *in vivo* data collection is challenging. We
233 initially collected data on five animals but only a limited number of trials from this study's three individuals
234 could be used for final analyses due to spatial (i.e. partial foot contacts) and temporal (i.e. starting data
235 collection after initial foot contact and/or terminating data collection before final foot contact) completeness
236 issues. We conducted a power analysis for a one-way ANOVA on our rhinoceros peak pressure data for
237 each foot, where omega-squared was used for the effect size, significance was set at 0.01 and power was
238 set at 0.8. The minimum number of rhinoceroses to achieve this power would be 8, 39, 29 and 13 for the
239 left forefoot, right forefoot, left hindfoot and right hindfoot datasets respectively. Considering accessibility
240 and experimental limitations, it will be difficult (if not impossible) to recruit enough rhinoceroses (>40
241 considering that some subjects would need to be discarded from any study) from the same captive setting
242 for a statistically robust experiment.

243 Habitat loss and poaching have brought many rhinoceros species, in particular the Javan and the Sumatran,
244 to the brink of extinction (Crosta et al., 2017). Despite on-going legal and conservation efforts to protect
245 rhinoceroses, the number of populations impacted by poaching has increased dramatically over the last two
246 decades, with South Africa being affected the most due to having the largest number of rhinoceroses in the
247 world (Charlton, 2017; Crosta et al., 2017). One of the measures in place to protect these animals from
248 extinction is to keep and breed them in captivity. While in captivity, they may develop foot disorders, in
249 particular chronic foot diseases, osteoarthritis, bone remodelling, osteitis-osteomyelitis, pododermatitis,
250 abscesses, and fractures (Galateanu et al., 2013; Jacobsen, 2002; Regnault et al., 2013; von Houwald and
251 Flach, 1998) that compromise animal welfare or even cause mortality due to being painful, progressive and

252   often untreatable. Even in wild rhinoceroses, there are reports of serious foot disease (Zainuddin et al.,
253   1990), and a high incidence of osteopathology appears to be an ancestral evolutionary trait for the lineage,
254   which may complicate efforts to improve the welfare of rhinoceroses (Stilson et al., 2016). To date, most
255   focus on appendicular pathologies in extant rhinoceroses have been on the feet, but the latter study's finding
256   that pathologies have been equally prevalent across the limbs throughout the ~50 million year history of
257   Rhinocerotidae raises questions of whether more proximal limb pathologies remain common but
258   overlooked in captive rhinoceroses. Follow-up studies should investigate this question and even integrate
259   it with biomechanical analyses to test whether some regional mechanical stresses are unusually high and
260   corresponding with locations predisposed to pathologies. Pond and Alexander (1992) used a very simple
261   analysis to estimate that femur safety factors were high in a galloping White rhinoceros but this method
262   certainly is imprecise, and stresses in the humerus or zeugopodial elements are unknown--- as are any joint
263   contact stresses, which should be more important for pathologies.

264   Disease management in large mammals such as elephants and rhinoceroses can be challenging and
265   examination using diagnostic approaches requires general anaesthesia or sedation, which can have negative
266   effects on the animal (Gage, 2006; Hittmair and Vielgrader, 2000; Siegal-Willott et al., 2012; von Houward
267   and Flach, 1998). These challenges, coupled with the fact that foot diseases may only clearly manifest
268   themselves when they have progressed to advanced stages, can make euthanasia an unavoidable outcome
269   (e.g. Jones, 1979; Mikota, 1999; Mikota et al., 1994). The causes of foot pathologies are multifactorial (e.g.
270   Csuti et al., 2001), but the biomechanical pressures imposed during locomotion presumably can promote
271   or worsen them. How can we thus protect rhinoceroses from developing foot diseases, or monitor treatment
272   vs. progression of chronic foot disease? An important step is to learn how rhinoceros feet function in
273   captivity. A valuable follow-on step would be to examine how husbandry conditions in captivity affect
274   innate foot function. Nevertheless, whilst we have a fair understanding of elephant foot pressures from
275   captive and semi-wild settings (Panagiotopoulou et al., 2012; 2016), here we have added new data on the
276   pressures that White rhinoceroses routinely apply to their feet during normal locomotion, and these give
277   tentative insights into not only basic biomechanics but also potential links of normal form and function vs.
278   mechanically-induced foot disease.

279

Conclusions

281   We conclude that there is tentative support for our hypothesis I, that peak locomotor pressures during
282   walking in White rhinoceroses are the lowest in the central and caudal parts of the foot at the locations of
283   the fat pad and its lobes, as in elephants. We also found support for our hypothesis II, that peak pressures
284   are equally concentrated around the horns/hooves and phalangeal pads of digits II-IV (unlike elephants)
285   instead of being concentrated more laterally onto digits III and IV (analogous to elephants). This finding
286   concurs with the incidence of osteopathologies, bolstering the proposition that there is a link between
287   locomotor pressures during walking and such pathologies (Regnault et al., 2013, 2017).

288

Acknowledgements

290   We thank the keepers and members of staff at the Colchester Zoo, UK for their assistance with the
291   experiments. We also thank RVC graduates Katherine Jones, Richard Harvey and Keri Holmes for
292   assistance with data collection. Thanks are due to Hyab Mehari Abraha from Monash University and the
293   Monash Bioinformatics Platform for technical support. We are also grateful for the two peer reviewers'
294   constructive critiques.

295

296   **Table 1**. Subject characteristics (*Ceratotherium simum*). Due to equipment calibration limitations,
297   absolute pressure values may be inaccurate (see Methods), but relative pressure values across subjects and
298   feet are expected to be reliably quantified.

299   **Figure 1.** Schematic illustration of the position of the pressure plates and the nine regions of interest
300   (ROI) during data collection. A. Image of Subject 3 walking on the pressure plate in the experimental
301   walkway. B. Schematic representation of the anatomical location of the nine (ROIs across the left
302   forefoot.

303   **Figure 2**. Scatter plot of peak foot pressure data from all three subjects at the nine regions of interest
304   (ROI) across the left forefoot, right forefoot, left hindfoot and right hindfoot respectively. Black line
305   represents the median pressure found at each ROI.

306   **Figure 3**. Peak pressure patterns during the whole stance phase of the left forefoot of subjects 1 (A, B)
307   and 2 (C-E).

308   **Figure 4**. Peak pressure patterns during the whole stance phase of the right forefoot of subjects 1 (A, B)
309   and 2 (C-F).

310   **Figure 5**. Peak pressure patterns during the whole stance phase of the left hindfoot of subjects 1 (A), 2
311   (B) and 3 (C).

312   **Figure 6**. Peak pressure patterns during the whole stance phase of the right hindfoot of subjects 1 (A, B)
313   and 2 (C).

314

315   **Supplementary Data 1:** Regional peak pressure data for all subjects and feet. Columns A-J show
316   respectively the file name (A), subject ID (B), foot ID (C: left forefoot = 1; right forefoot = 2; left
317   hindfoot = 3; right hindfoot = 4); ROI (D; also see Figure 1); peak pressure data in N cm^{-2} (E); walking
318   speed in m s^{-1} (F); Shoulder height in metres (G); Froude number (H); Age (I; Adult=1; juvenile=2);
319   Body mass estimate in kg (J; 1 = 2500; 2 = 1000). Some trials were excluded from further analyses due to
320   being temporally incomplete. These are: [FORE LEFT: subject 1, trial 028_img001], [FORE RIGHT:
321   subject 3, trial 033_img004; subject 3, trial 035_img003], HIND LEFT: subject 3, trial 010_img003],
322   [HIND RIGHT: subject 3, trial 041_img006; subject 1, trial 001_img002; subject 1, trial 013_img005].

323   **Supplementary Figure S1**: Image time series of the COP trajectories (light grey) for the left forefoot of
324   subject 1 (010_img002 [A] and 027_img002 [B]).

325   **Supplementary Figure S2**: Image time series of the COP trajectories (light grey) for the left forefoot of
326   subject 2 (trials 018_img005 [A], 021_img005 [B] and 031_img002 [C]).

327   **Supplementary Figure S3**: Image time series of the COP trajectories (light grey) for the right forefoot of
328   subject 1 (trials 27_10_035_img002 [A] and 27_10_img002 [B]).

329   **Supplementary Figure S4**: Image time series of the COP trajectories (light grey) for the right forefoot of
330   subject 2 (trials 004_img007 [A], 009_img006 [B], 011_img004 [C] and 033_img003 [D]).

331   **Supplementary Figure S5**: Image time series of the COP trajectories (light grey) for the left hindfoot of
332   subject 1 (trials 27_10_038_img005 [A] and 014_img002 [B]).

333   **Supplementary Figure S6:** Image time series of the COP trajectories (light grey) for the left hindfoot of
334   subject 2 (trial 026_img004).

335   **Supplementary Figure S7**: Image time series of the COP trajectories (light grey) for the left hindfoot of
336   subject 3 (trial 034_img003).

337 **Supplementary Figure S8**: Image time series of the COP trajectories (light grey) for the right hindfoot of
338 subject 1 (trials 27_10_037_img003 [A] and 032_img003 [B]) and subject 2 (trial 27_10_019_img001 [C]).

339

340 **References**

341 Alexander RM, Pond CM. 1992. Locomotion and bone strength of the white rhinoceros, *Ceratotherium*
342 *simum*. Journal of Zoology 227(1): 63-69.

343

344 Alexander RMN, Jayes AS. 1983. A dynamic similarity hypothesis for the gaits of quadrupedal
345 mammals. Journal of Zoology 201: 135–152. (doi:10.1111/j.1469-7998.1983.tb04266.x)

346

347 Charlton RW. 2017. Death and destruction: insight into the rhino poaching epidemic in South Africa.
348 Illinois State University. *Theses and Dissertations*, 661. https://ir.library.illinoisstate.edu/etd/661

349

350 Chi KJ, Roth VL. 2010. Scaling and mechanics of carnivoran footpads reveal the principles of footpad
351 design. Journal of the Royal Society Interface 7(49): 1145-1155

352

353 Crosta A, Sutherland K, Talerico C. 2017. Grinding rhino: An undercover investigation on rhino horn
354 trafficking in China and Vietnam. Elephant Action League Report.

355

356 Csuti B, Sargent EL, Bechert US. 2001. *The Elephant's Foot: Prevention and Care of Foot Conditions in*
357 *Captive Asian and African Elephants*. Ames, IA: Iowa State University Press.

358

359 Dudley RJ, Wood SP, Hutchinson JR, Weller R. 2014. Radiographic protocol and normal anatomy of the
360 hind feet in the white rhinoceros (*Ceratotherium simum*). Veterinary Radiology & Ultrasound 56 (2):
361 124-132. (doi.org/10.1111/vru.12215)

362

363 Flach E, Walsh T, Dodds J, White A, Crowe O. 2003. Treatment of osteomyelitis in a greater one-horned
364 rhinoceros (*Rhinoceros unicornis*). Verhandlungsbericht des 41 Internationalen Symposiums über die
365 Erkrankungen der Zoo-und Wildtiere 28, 1-7.

366

367 Fowler ME, Mikota SK. 2006. *Biology, Medicine, and Surgery of Elephants*. Ames, IA: Blackwell
368 Publishing Ltd.

369

370 Gage L. 2006. Radiology. In: Fowler ME, Mikota SK, editors. *Biology, Medicine, and Surgery of*
371 *Elephants*. Ames, IA: Blackwell Publishing. pp. 192–197.

372

373 Galateanu G, Hildebrandt TB, Maillot A, Etienne P, Potier R, Mulot B, Saragusty J, Hermes R. 2013.
374 One small step for rhinos, one giant leap for wildlife management- imaging diagnosis of bone pathology
375 in distal limb. Plos One 8(7): e68493. (doi: 10.1371/journal.pone.0068493)

376

377 Groves CP. 1972. *Ceratotherium simum*. Mammalian Species 8: 1-6.

378

379 Harrison T, Stanley B, Sikarskie J, Bohart G, Ames N, Tomlian J, Marquardt M, Marcum A, Kiupel M,
380 Sledge D, Agnew D. 2011. Surgical amputation of a digit and vacuum-assisted-closure (V.A.C.)
381 management in a case of osteomyelitis and wound care in an eastern black rhinoceros (*Diceros bicornis*
382 *michaeli*). Journal of Zoo and Wildlife Medicine 42: 317–321.

383

384 Hillman-Smith, AKK, Owen-Smith N, Anderson JL, Hall-Martin AJ, Selaladi JP. 1986. Age estimation
385 of the white rhinoceros (*Ceratotherium simum*). Journal of Zoology 210 (3): 355-377.
386 (doi: 10.1111/j.1469-7998.1986.tb03639.x)

387

388 Hittmair KM, Vielgrader HD. 2000. Radiographic diagnosis of lameness in African elephants (*Loxodonta*
389 *africana*). Veterinary Radiology & Ultrasound 41 (6):511-515.

390

391 Hutchinson JR, Delmer C, Miller CE, Hildebrandt T, Pitsillides AA, Boyde AJ. 2011. From flat foot to
392 fat foot: the structure, ontogeny, function and evolution of elephant 'sixth toes'. Science 344: 1699–1703.
393 (doi:10.1126/science.1211437)

394

395 Jacobsen J. 2002. A Review of Rhino Foot Problems. In: *Proceedings of the 2nd Rhino Keepers'*
396 *Workshop 2001*. Zoological Society of San Diego, San Diego, California. Pp. 56–59.

397

398 Jones D. 1979. The husbandry and veterinary care of captive rhinoceroses. International Zoo Yearbook
399 19: 239–250.

400

401 Lord M, Reynolds DP, Hughes JR. 1986. Foot pressure measurement: a review of clinical findings.
402 Journal of Biomedical Engineering 8: 283-294.

403

404 Mariappa D. 1986. *Anatomy and Histology of the Indian Elephant*. Oak Park, MI: Indira Publishing
405 House.

406

407 Michilsens F, Aerts P, Van Damme R, D'Août K. 2009. Scaling of plantar pressures in mammals. Journal
408 of Zoology 279(3): 236-242.

409

410   Mikota SK, Sargent EL, Ranglack GS. 1994. *Medical Management of the Elephant*. Indira Publishing
411   House, West Bloomfield, Michigan.

412

413   Mikota SK. 1999. Diseases of the elephant: a review. In Erkrankungen der Zootiere: Verhandlungsbericht
414   des 39. Internationalen Symposiums uber die Erkrankungen der Zoo undWildtiere, pp. 1–15.

415

416   Miller MA, Hogan JN, Meehan CL. 2016 Housing and demographic risk factors impacting foot and
417   musculoskeletal health in African elephants (*Loxodonta africana*) and Asian elephants (*Elephas
418   maximus*) in North American Zoo. PLoS ONE 11, e0155223. (doi:10.1371/journal.pone.0155223)

419

420   Neuville H. 1935. Sur quelques caractères anatomiques du pied des éléphants. Archives du Muséum
421   d'Histoire Naturelle, Paris, 6 e Série 13: 111–183.

422

423   Owen-Smith RN. 1992. *Megaherbivores: The Influence of Very Large Body Size on Ecology*. Cambridge
424   university press.

425

426   Panagiotopoulou O, Pataky TC, Hutchinson JR. 2019. "Supplementary data 2" containing raw foot-roll
427   off dataset from all trials of pressure pad experiments with White rhinoceroses. doi:
428   10.6084/m9.figshare.7608797 From the study by Panagiotopoulou O, Pataky TC, Hutchinson JR. In
429   review. Foot pressure distribution in White rhinoceroses (*Ceratotherium simum*) during walking. PeerJ.

430

431   Panagiotopoulou O, Pataky TC, Day M, Hensman MC, Hensman S, Hutchinson JR, Clemente CJ. 2016.
432   Foot pressure distributions during walking in African elephants (*Loxodonta africana*). Royal Society
433   Open Science 3:160203 (http://dx.doi.org/10.1098/rsos.160203)

434

435   Panagiotopoulou O, Pataky TC, Hill Z, Hutchinson JR. 2012. Statistical parametric mapping of the
436   regional distribution and ontogenetic scaling of foot pressures during walking in Asian elephants (*Elephas
437   maximus*). Journal of Experimental Biology 215: 1584–1593 (doi:10.1242/jeb.065862)

438

439   Prothero DR. 2005. *Evolution of North American Rhinoceroses*. Cambridge University Press.

440

441   Regnault S, Dixon JJI, Warren-Smith C, Hutchinson JR, Weller R. 2017. Skeletal pathology and variable
442   anatomy in elephant feet assessed using computed tomography. PeerJ 5:e2877 (doi:10.7717/peerj.2877)

443

444   Regnault S, Hermes R, Hildebrandt T, Hutchinson JR, Weller R. 2013. Osteopathology in the feet of
445   rhinoceroses: lesion type and distribution. Journal of Zoo and Wildlife Medicine 44: 918–927 (doi:
446   10.1638/2012-0277R1.1 PMID: 24450050)

447

448 Siegal-Willott JL, Alexander A, Isaza R. 2012. Digital Radiography of the Elephant Foot. In: Fowler ME,
449 Miller RE, editors. *Zoo and Wild Animal Medicine, Current Therapy*. St. Louis, Missouri: Elsevier
450 Saunders. pp. 515–523

451

452 Stilson KT, Hopkins SSB, Davis EB. 2016. Osteopathology in Rhinocerotidae from 50 million years to
453 the present. PLoS ONE 11(2): e0146221 (doi:10.1371/journal.pone.0146221)

454

455 Van der Tol PPJ, Metz JHM, Noordhuizen-Stassen EN, Back W, Braam CR, Weijs WA. 2002. The
456 pressure distribution under the bovine claw during square standing on a flat substrate. Journal of Dairy
457 Science 85:1476-1481.

458

459 Van der Tol PPJ, Metz JHM, Noordhuizen-Stassen EN, Back W, Braam CR, Weijs WA. 2003. The
460 vertical ground reaction force and the pressure distribution on the claws of dairy cows while walking on a
461 flat substrate. Journal of Dairy Science 86:2875-2883.

462

463 Van der Tol PPJ, Van Der Beek SS, Metz JHM, Noordhuizen-Stassen EN, Back W, Braam CR, Weijs
464 WA. 2004. The effect of preventive trimming on weight bearing and force balance on the claws of dairy
465 cattle. Journal of Dairy Science 87:1732-1738.

466 von Houwald F, Flach EJ. 1998. Prevalence of chronic foot disease in captive greater one-horned
467 rhinoceros (*Rhinoceros unicornis*). EAZWV Scientific Meeting 2: 323-327.

468

469 von Houwald F, Guldenschuh G. 2002. *Husbandry manual for the greater one-horned or Indian
470 rhinoceros (Rhinoceros unicornis)* Linne, 1758. Basel Zoo, Basel, Switzerland.

471

472 von Houwald F. 2001. Foot problems in Indian rhinoceroses (*Rhinoceros unicornis*) in zoological
473 gardens: macroscopic and microscopic anatomy, pathology, and evaluation of the causes. Ph.D.
474 dissertation, University of Zurich, Zurich, Switzerland.

475

476 Weissengruber GE, Egger GF, Hutchinson JR, Groenewald HB, Elsasser L, Famini D, Forstenpointner G.
477 2006. The structure of the cushions in the feet of African elephants (*Loxodonta africana*). Journal of
478 Anatomy 209: 781–792 (doi:10.1111/j. 1469-7580.2006.00648.x)

479

480 Zainuddin ZZ, Abdullah MT, Shamsuddin M, Suri M. 1990. The husbandry and veterinary care of
481 captive Sumatran rhinoceros at Zoo Melaka, Malaysia. Malayan Nature Journal (Malaysia).

482

483

484

485

486

487

488

489

Subject characteristics (*Ceratotherium simum*).

Due to equipment calibration limitations, absolute pressure values may be inaccurate (see Methods), but relative pressure values across subjects and feet are expected to be reliably quantified.

2
3

	Subject 1	Subject 2	Subject 3
Age	Adult	Juvenile	Adult
Sex	Female	Female	Female
Body mass (kg)- estimated	2500	1000	2500
Shoulder height (m)	1.5	0.65	1.42
Mean Froude number	0.014	0.001	0.054
Mean velocity (ms^{-1})	0.46	0.60	0.87
Mean maximum pressure (N cm^{-2}) Fore Left 1	23	13	No spatially or temporally complete data
Mean maximum pressure (N cm^{-2}) Fore Right 2	28	9	No spatially or temporally complete data
Mean maximum pressure (N cm^{-2}) Hind Left 3	18	4	12
Mean maximum pressure (N cm^{-2}) Hind Right 4	2	No spatially or temporally complete data	No spatially or temporally complete data
Number of steps	4	3	1
Trials (multiple steps)	60	38	115
Steps, Fore Left	29	17	51
Steps, Fore Right	37	12	47
Steps, Hind Left	15	9	13
Steps, Hind Right	10	13	12

6
7
8
9
10
11

Figure 1

Schematic illustration of the position of the pressure plates and the nine regions of interest (ROI) during data collection.

A. Image of Subject 3 walking on the pressure plate in the experimental walkway. B. Schematic representation of the anatomical location of the nine (ROIs across the left forefoot.)
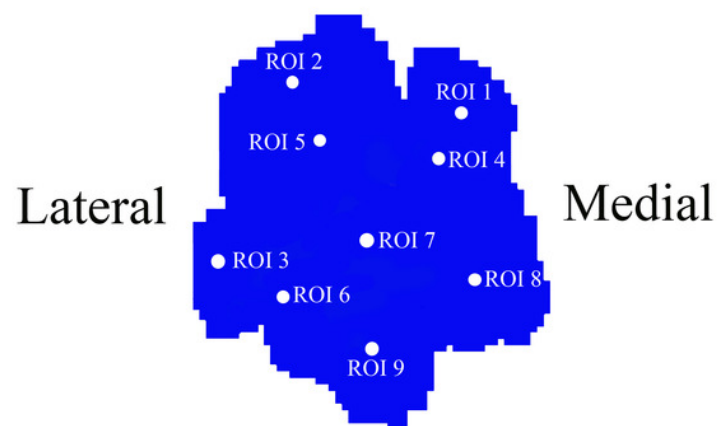
Scatter plot of peak foot pressure data from all three subjects at the nine regions of interest (ROI) across the left forefoot, right forefoot, left hindfoot and right hindfoot respectively.

Black line represents the median pressure found at each ROI.
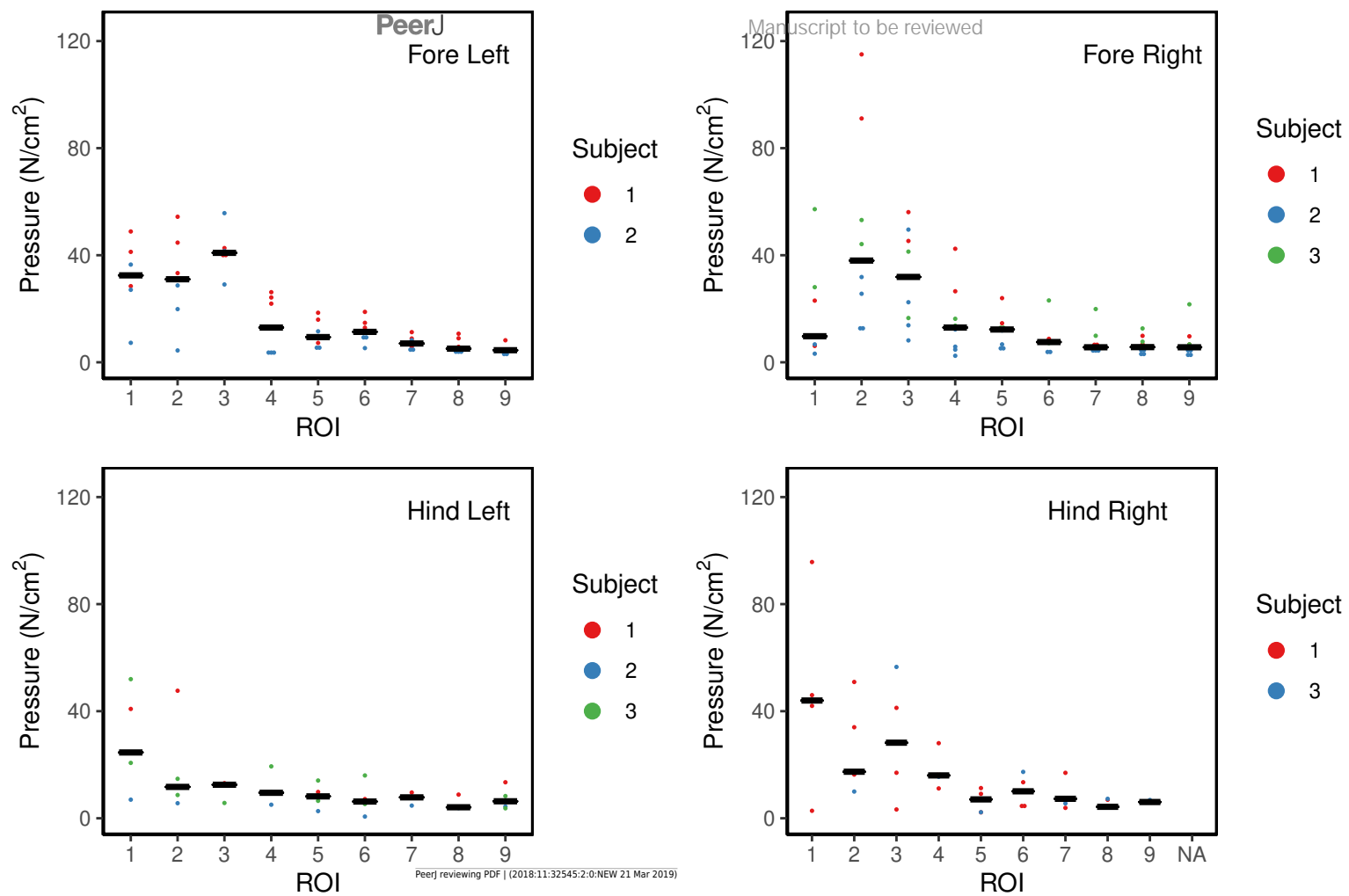
Figure 3

Peak pressure patterns during the whole stance phase of the left forefoot of subjects 1 (A, B) and 2 (C-E).

Fore Left
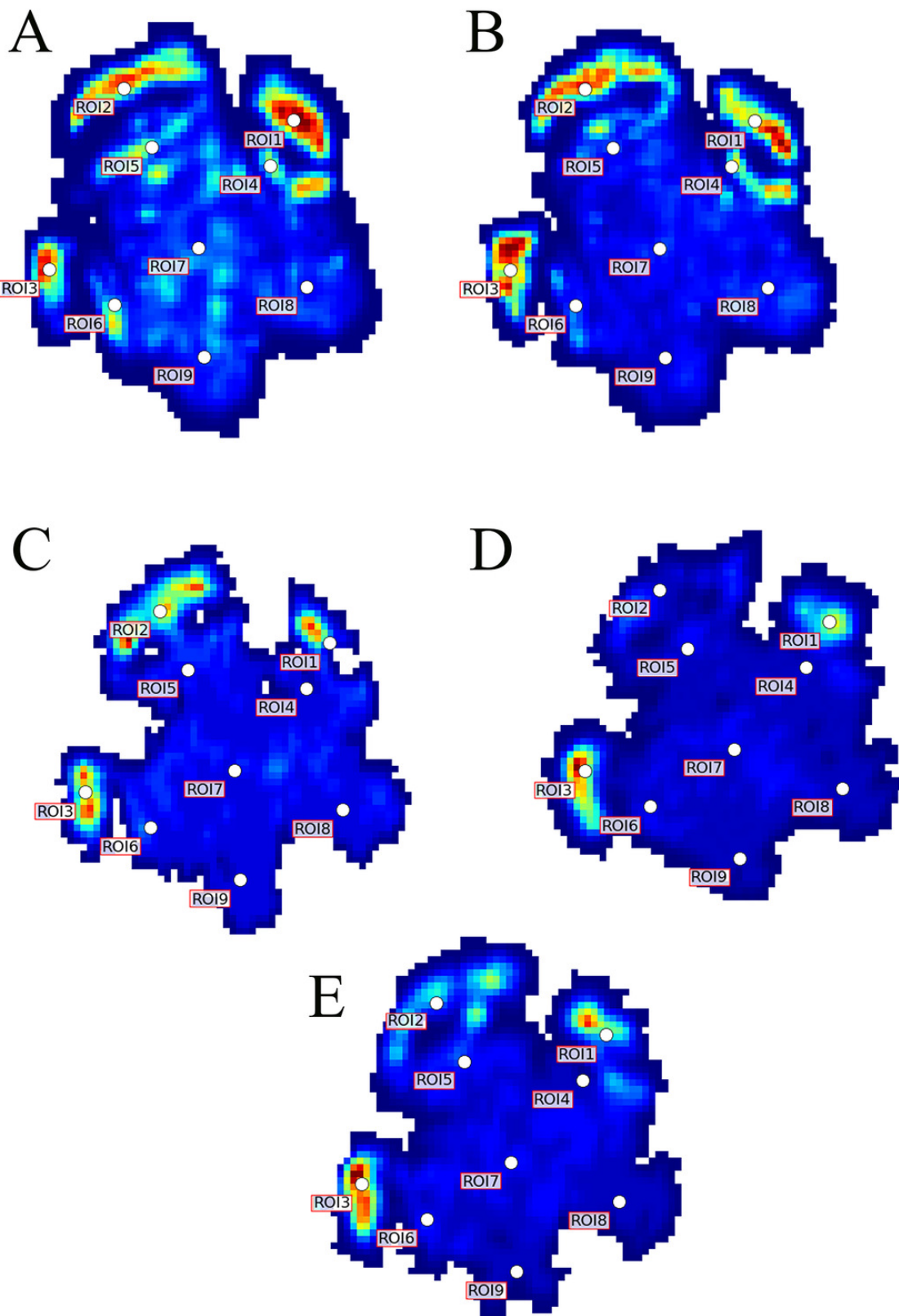
Figure 4

Peak pressure patterns during the whole stance phase of the right forefoot of subjects 1 (A, B) and 2 (C-F).

Fore Right
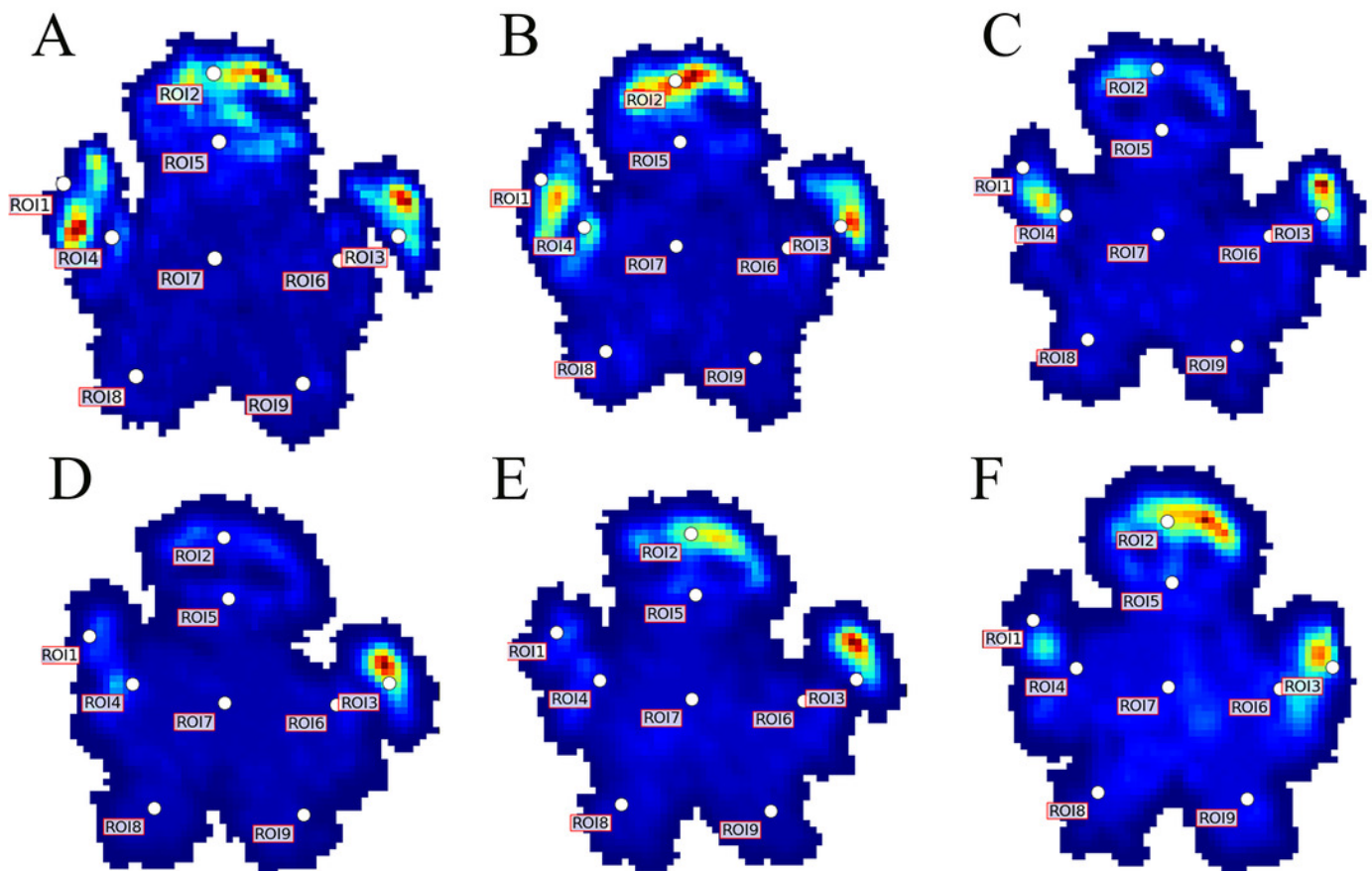
Figure 5

Peak pressure patterns during the whole stance phase of the left hindfoot of subjects 1 (A), 2 (B) and 3 (C).

Figure 6

Peak pressure patterns during the whole stance phase of the right hindfoot of subjects 1 (A, B) and 2 (C).